



Large- and small-scale periodicities in the mesosphere as obtained from variations in O₂ and OH nightglow emissions

Ravindra P. Singh^{1,2} and Duggirala Pallamraju¹

¹Space and Atmospheric Sciences Division, Physical Research Laboratory, Ahmedabad, India

²Department of Physics, Sardar Patel University, Vallabh Vidyanagar, India

Correspondence to: Ravindra P. Singh (ravindra@prl.res.in)

Received: 28 July 2016 – Revised: 9 January 2017 – Accepted: 30 January 2017 – Published: 21 February 2017

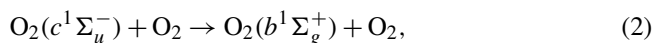
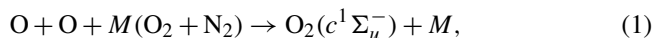
Abstract. Using 3 years (2013–2015) of O₂(0–1) and OH(6–2) band nightglow emission intensities and corresponding rotational temperatures as tracers of mesospheric dynamics, we have investigated large- and small-timescale variations in the mesosphere over a low-latitude location, Gurushikhar, Mount Abu (24.6° N, 72.8° E), in India. Both O₂ and OH intensities show variations similar to those of the number of sunspots and F10.7 cm radio flux with coherent periodicities of 150 ± 2.1 , 195 ± 3.6 , 270 ± 6.4 , and 420 ± 14.8 days, indicating a strong solar influence on mesospheric dynamics. In addition, both mesospheric airglow intensities also showed periodicities of 84 ± 0.6 , 95 ± 0.9 , and 122 ± 1.3 days which are of atmospheric origin. With regard to the variability of the order of a few days, O₂ and OH intensities were found to be correlated, in general, except when altitude-dependent atmospheric processes were operative. To understand mesospheric gravity wave behavior over the long term, we have carried out a statistical study using the periodicities derived from the nocturnal variations in all four parameters (O₂ and OH intensities and their respective temperatures). It was found that the major wave periodicity of around 2 h duration is present in all the four parameters. Our analyses also reveal that the range of periods in O₂ and OH intensities and temperatures is 11 to 24 and 20 to 60 min, respectively. Periods less than 15 min were not present in the temperatures but were prevalent in both emission intensities. No seasonal dependence was found in either the wave periodicities or the number of their occurrence.

Keywords. Atmospheric composition and structure (airglow and aurora) – meteorology and atmospheric dynamics (middle atmosphere dynamics) – ionosphere (instruments and techniques)

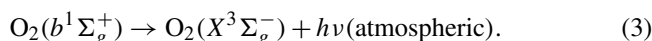
1 Introduction

Airglow emissions are known to play an important role in the studies of the dynamical processes that occur in the earth's atmosphere. This is because the variability in photochemical processes that bring about the variations in the corresponding intensities is directly related to variations in atmospheric temperature and density of the reactants. The large- and small-scale variations in the mesospheric intensities and temperatures can be due to either solar flux variation or atmospheric dynamical processes which are driven by gravity waves (GWs), tides, and planetary waves. The observed variability in mesospheric emissions is a result of the convolved behavior between the solar forcing and atmospheric dynamics. We have used O₂(0–1) atmospheric and OH(6–2) band emission intensities that emanate from approximately 94 and 87 km, respectively, and corresponding temperatures to understand the solar and dynamical effects on these parameters.

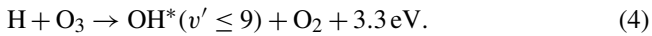
Production mechanisms that give rise to these band emissions in the mesosphere are summarized below. The O₂ atmospheric band emission is a two-step process with a three-body collision (Barth mechanism) required to place the O₂ in an excited state (e.g., Torr et al., 1985),



and the atmospheric O₂ band emission results from de-excitation of the O₂(*b*¹Σ_g⁺) state,



The mechanism for OH Meinel band emission is given by (e.g., Meriwether Jr., 1989, and references therein):



This OH* de-excites to ground state at various vibrational levels. In this study, we have considered O₂(0–1) atmospheric band emissions centered at 866.0 and 868.0 nm and OH(6–2) Meinel band emissions centered at 840.0 and 846.5 nm wavelengths. From Eqs. (1) to (4) it can be seen that the O₂ and OH nightglow emission intensities are related to the concentrations of atomic oxygen and ozone and hence to the extreme ultraviolet (EUV) solar energy input that is responsible for their photochemical production. Therefore, these emissions are expected to show variations with the EUV solar energy input and hence with solar activity. However, quantitative understanding of solar effects on mesospheric parameters is far from complete. The temporal variations of various timescales can be investigated by carrying out high-cadence and systematic long-term ground-based measurements of airglow emission intensities and temperatures. In the mesopause region the response to solar activity is small in comparison to the upper thermosphere, where strong absorption of solar EUV causes strong solar forcing (e.g., Laskar et al., 2015). Solar effects on the variation in mesospheric emissions and temperatures have been studied by different investigators using ground-based data. For example, Wiens and Weill (1973) showed that OH(9–3) band nightglow intensity follows the variation in solar activity; Batista et al. (1994) showed that OH(9–4) band nightglow intensity had a positive correlation with the solar 10.7 cm radio flux index (F10.7). However, Scheer et al. (2005) showed that there was no correlation of OH(6–2) band nightglow intensities and temperatures with solar radio flux, but they found a moderate positive correlation with O₂(0–1) nightglow intensity and temperatures. Pertsev and Perminov (2008) showed that the response of O₂ and OH nightglow intensity to solar 10.7 cm radio flux could reach 40%/100 solar flux units (sfu) and 30%/100 sfu, respectively. The response of the mean annual OH temperature to solar activity is shown to be different in different works, for example around 1 K/100 sfu (Scheer et al., 2005), 4.5 K/100 sfu (Pertsev and Perminov, 2008), and 11 K/100 sfu (Clemesha et al., 2005). As discussed above, experimental results on solar-cycle-related effects on the magnitudes of intensity and temperature over low-latitude mesosphere–lower thermosphere (MLT) region are ambiguous. In this study a clear imprint of solar effect in the mesospheric nightglow intensity and temperature variations is presented.

In addition to the large-scale effect on the mesospheric airglow intensities and temperatures it is also important to understand the effect of oscillations of short timescale (GW regime) on these parameters. The atmospheric dynamics varies with latitude, longitude, seasons, topography, etc.; therefore, their effects on the mesospheric airglow intensities and temperatures are expected to be different at different locations. GWs play an important role in the MLT en-

ergetics and dynamics since they act as significant source of momentum and energy flux in this region. Further, the GWs in the mesosphere are significantly affected by tropospheric cyclones, as shown in a recent study by Singh and Pallamraju (2016), wherein unambiguous evidence was obtained for the propagation of waves from the troposphere to the mesosphere during cyclone Nilofar, which occurred in October 2014 in the Arabian Sea, to the west of our optical observational location of Gurushikhar (24.6° N, 72.8° E), in India. Therefore, gravity wave studies at various locations over different time durations have formed one of the important topics of investigation (e.g., Fritts and Alexander, 2003). Many ground-based techniques have been used to study GW activities in the MLT region, involving, for example, photometers, spectrometers, imagers, radars, and lidars. A few of the results obtained by various techniques are described here to provide a broad context to understand the results reported in this work. Taylor et al. (1997) reported an anisotropic distribution in the directions of wave propagation during equinoxes over low latitude from Alcântara, Brazil (2.3° S, 44.5° W). Nakamura et al. (1999) reported that the GW propagations over midlatitudes (Shigaraki; 35° N, 136° E; Japan) show seasonal variation with an eastward/westward preference in summer/winter. Similar behavior was seen over another mid-latitude location (Mt. Bohyun; 36.2° N, 128.9° E; Korea; Kim et al., 2010), wherein it was found that GWs tended to propagate westward during fall and winter, and eastward during spring and summer. In contrast, Ejiri et al. (2003) showed that GWs propagated northward and northeastward in summers and westward at Rikubetsu (43.5° N, 143.8° E), and southwestward at Shigaraki (34.9° N, 136.1° E) in winters during a different epoch. Using OH airglow imager data from Tirunelveli (8.7° N, 77.8° E), Lakshmi Narayanan and Gurubaran (2013) reported that nearly half of the high-frequency GWs were evanescent, with more occurrences in solstices as compared to equinoxes and showed predominant meridional propagation throughout the year. Sivakandan et al. (2016) reported that GWs propagate mostly northward of Gadanki (13.5° N, 79.2° E). Most of earlier works have concentrated on the directions of propagations of gravity waves as seen in the imagers. The present work, in contrast, is focused on understanding the wave periodicities and their variations over long and short timescales.

In order to characterize the various periodicities, from long to short timescales that are prevalent in the mesosphere, we have investigated the mesospheric O₂(0–1) and OH(6–2) band nightglow emission intensities and their rotational temperatures obtained over a 3-year (2013–2015) duration from a low-latitude location, Gurushikhar, Mount Abu, in India. From the long-term observations, it was found that the solar effects and local dynamical processes were both present simultaneously in O₂ and OH emission intensities and temperatures. We have also studied the correlation between O₂ and OH intensities along with the variability in the sunspot

number (SSN) and solar F10.7 cm flux. The GWs derived from the nocturnal variations in these parameters were also investigated and are described in the following sections.

2 Instrumentation and data used

Our near-infrared imaging spectrograph (NIRIS) was developed in-house and has been operating from a low-latitude location (Gurushikhar, Mount Abu; 24.6° N, 72.8° E), in India since January 2013. NIRIS provides O₂(0–1) atmospheric and OH(6–2) Meinel band nightglow emission spectra with a spectral resolution of 0.78 nm in a large field of view of around 80° with a data cadence of 5 min. The details of the NIRIS and the methodology used to obtain nocturnal intensities and of deriving mesospheric temperatures using rotational line ratios of O₂ and OH band emissions can be found elsewhere (Pallamraju et al., 2014; Singh and Pallamraju, 2015). The O₂ and OH emission intensities are determined by integrating the nightglow brightness over 1.2 nm centered at each emission wavelength and are given in arbitrary units.

Figure 1 shows total observational duration for a given night starting from 1 January 2013 to 21 November 2015, corresponding to day of year (DOY) 1 to 1055. The spectral images are checked visually for their quality. In addition, in this study we have considered only those nights for which the nightly observational duration is greater than 3 h. After implementing all these conditions there were a total of 437 nights of observations available for detailed investigations. The average duration of the observation per night is 8.4 ± 2.3 h, which is based on more than 35 000 clear spectra obtained from NIRIS. The variations in the data duration and data gaps seen in Fig. 1 are due to the changes in phases of moon, seasons, and cloud cover. We get maximum durations in observation around the new moon phase for cloud-free nights, and these conditions prevail mostly during the winter season. There were two large data gaps during DOY 455 to 652 and 893 to 1003, which were resulted from technical difficulties with the data acquisition system of the NIRIS.

3 Results and discussions

Variations in the O₂ and OH emission intensities are presented in Fig. 2a and b starting from 1 January 2013 (DOY 1). The O₂(0–1) atmospheric band and OH(6–2) Meinel band intensities are obtained by taking the mean of 866 and 868 nm emissions and mean of P₁(2) and P₁(4) rotational line intensities at 840.0 and 846.5 nm emissions. These two sets of intensities of the rotational lines of O₂ and OH band emissions are also used to derive the corresponding rotational temperatures at those altitudes. The nightly mean values for O₂ and OH emission intensities (IO₂ and IOH) are shown in magenta and blue and the spread in the nightly values is shown in pink and sky blue, respectively. As will be shown below, the large spreads in the nocturnal O₂ and OH emission intensity vari-

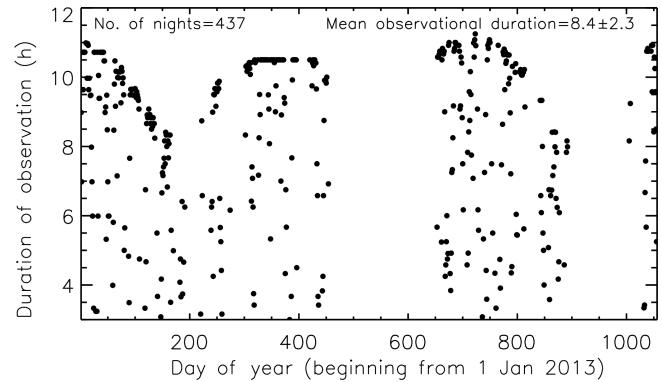


Figure 1. Details of the duration of observations obtained from the near-infrared imaging spectrograph (NIRIS) at Gurushikhar, Mount Abu (24.6° N, 72.8° E), in India. The durations of observations per night are shown as a function of day of year (DOY); DOY 1 corresponds to 1 January 2013.

ations in a given night signify the presence of GW-type oscillations. These emissions also show large time period variations which seem to be due to the seasonal and solar-cycle-related effects. In order to assess the effect of solar influence on the O₂ and OH intensities, the daily mean SSN and solar 10.7 cm radio flux are considered and are shown in Fig. 2c. The temperatures derived using O₂(0–1) and OH(6–2) band emission intensities (TO₂ and TOH) are shown in Fig. 2d and e (wherein we have used the same color codes as used for the intensities in Fig. 2a and b). Similar to the variations in emission intensities, temperatures at both altitudes show both small- and large-timescale fluctuations. A closer look at Fig. 2a–e shows that the response of solar effects is much more pronounced in intensities as compared to the temperatures. For example, the noticeable reductions in intensities seen during DOY 1–50 (January and February 2013) and in February and March 2015 (DOY 760–800) match quite well with those of the SSN and F10.7. However, the variations in temperatures at both altitudes do not show any visible similarity during these periods in comparison to the nightglow emission intensities. It has been shown recently that the responses to the tropical-cyclone-generated GWs in the mesospheric nightglow intensities were better than those in temperatures (Singh and Pallamraju, 2016).

All the six parameters shown in Fig. 2 have been subjected to spectral analyses to obtain the periodicities that are present in the data. As discussed earlier, the optical data obtained from the ground are not equally spaced in time; therefore, Lomb–Scargle periodogram analysis (Lomb, 1976; Scargle, 1982) has been carried out, which takes care of unequal spacing in the data. As seen in Fig. 2, there are two large data gaps in the ground-based observations. Therefore, we have considered two periods (DOY 1 to 454 and DOY 653 to 893) wherein we have continuous ground-based observation. In addition, we have also considered the total data from DOY 1

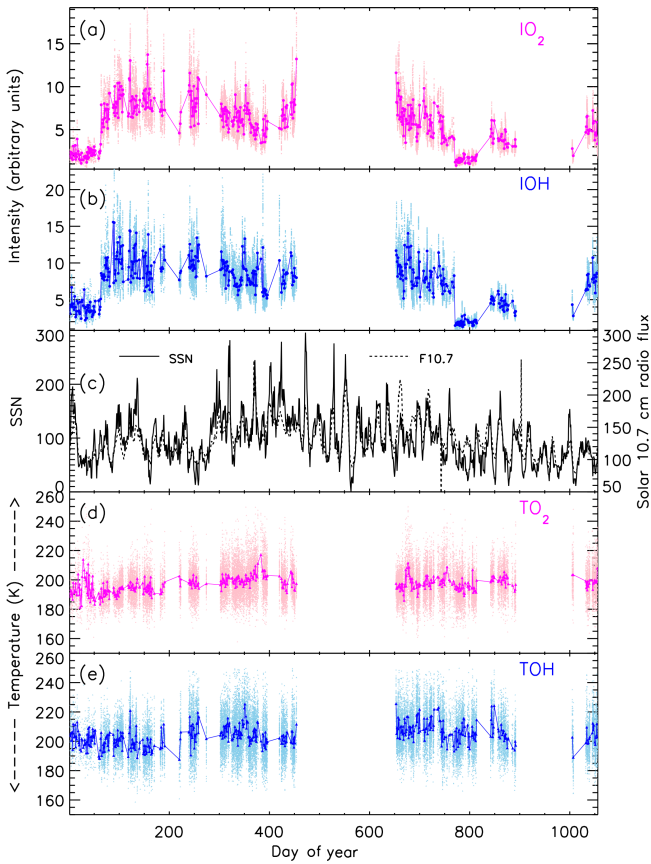


Figure 2. (a, b) Nightly mean O₂ and OH intensity variations measured by NIRIS at Mount Abu which originate from 94 and 87 km altitude, respectively. The ranges in the nocturnal variations are also shown. (c) Variations in daily mean sun spot numbers and F10.7 for all days (DOY 1 to 1055). (d, e) Nightly mean variations in the corresponding O₂ and OH temperatures along with their nightly range.

to 1055. It should be mentioned here that even though the ground-based observations suffer from gaps in the data, we have considered continuous data of solar parameters (SSN and F10.7) for obtaining information on the solar oscillations existing in that duration.

The periodicities of the variations that are obtained from Lomb–Scargle periodogram analysis in the O₂ and OH intensities and their corresponding temperatures, SSN and F10.7 are all shown in Fig. 3. The horizontal lines in all the panels in Fig. 3 show the false-alarm levels (FALs) related to the confidence level of 90 % for the spectral analysis as obtained above. As can be seen from Fig. 3a, periodicities obtained from first 455 days of data (from DOY 1 to 454) in IO₂ are 90 ± 1.5, 120 ± 2.5, 180 ± 4.9 days; in IOH 120 ± 2.5 and 180 ± 4.7 days; and in TOH 120 ± 2.4 days. The uncertainty in the peak value of a given period shown above is calculated using the following relation (Bretthorst, 1988):

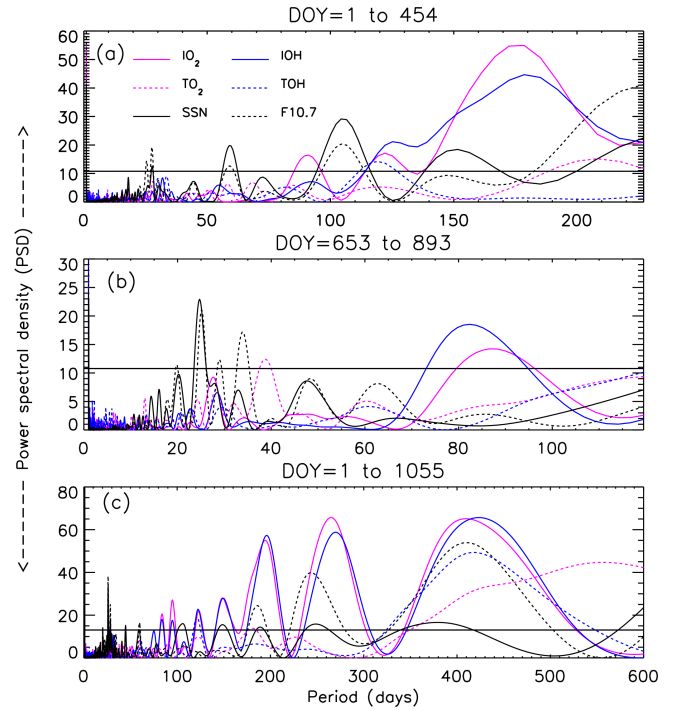


Figure 3. (a) Lomb–Scargle periodograms of the O₂ and OH intensities and corresponding temperatures for the first 455 days of observations (DOY 1 to 454). Power spectral density (PSD) along with the 90 % false-alarm level (FAL) is shown for different periods of atmospheric nightglow and solar parameters. (b) Significant periodicities obtained using Lomb–Scargle periodogram analysis of 241 days of data (DOY 653 to 893). (c) Similar to (a, b) but for 1056 days of optical observations (DOY 1 to 1055). It should be mentioned here that, for solar parameters, continuous data without any gaps are considered. It is striking to note that, in addition to atmospheric periodicities that are present in the mesospheric intensity and temperature variations, several coherent periods are present in the O₂ and OH intensities and temperatures showing commonality with those obtained from SSN and F10.7.

$$\delta f = \frac{1.1\sigma}{A \cdot T_{\text{total}} \cdot \sqrt{N}} \text{ Hz}, \tag{5}$$

where f ($= 1/\tau$) is the wave frequency, with τ being the wave period; T_{total} is the total duration of observation; A is the amplitude of the signal; N is the number of measurements; and σ is the standard deviation of the noise after the signal has been subtracted. For the same duration the periodicities in the solar parameters are found to be 27 ± 0.06, 58 ± 0.3, 105 ± 0.9, 150 ± 1.9 (in SSN) and 27 ± 0.06, 58 ± 0.3, 105 ± 0.9 (in F10.7 cm flux) days (Fig. 3a). The reason behind the presence of these periodicities in SSN and F10.7 solar flux is the internal magnetic dynamo action in the solar interior. It has been shown that some of these periods are present in the solar magnetic flux variations during solar cycle 24 and may differ from year to year (Chowdhury

et al., 2015). Hence, it can be seen from Fig. 3a that the 90- and 120/180-day oscillations that are present in mesospheric intensity and temperature variations are of atmospheric (seasonal/semiannual) origin. Figure 3b shows the periodicities obtained from 241 days of data (DOY 653 to 893) in IO_2 , IOH, and TO_2 as 85 ± 3.7 , 85 ± 3.7 , and 38 ± 0.7 days, respectively. Figure 3b also shows the presence of 27-day solar periods in SSN and F10.7. The 85-day period seen in IO_2 and IOH is due to seasonal variations. Several significant periodicities in mesospheric intensities and temperatures that are present in 1056 days (DOY 1 to 1055) of data are shown in Fig. 3c. IO_2 and IOH show the presence of common periodicities of around 84 ± 0.6 , 95 ± 0.9 , 122 ± 1.3 , 150 ± 2.1 , 195 ± 3.6 , 270 ± 6.4 , and 420 ± 14.8 days. In addition, TO_2 and TOH also show the presence of periodicities of 420 ± 14.8 , 122 ± 1.4 and 420 ± 14.8 days. Figure 3c also shows the periodicities present in the solar variations, which are 27 ± 0.02 , 58 ± 0.08 , 105 ± 0.3 , 150 ± 0.5 , 190 ± 0.9 , 245 ± 1.4 , 380 ± 3.3 , and 410 ± 3.9 days. Results from spectral analyses of solar flux and SSN data showing the presence of periods around 150, 190, 245, and 410 days with significant power indicate that similar periods observed in optical emissions could be due to solar influences. There could also be contributions from semi-annual oscillation (SAO) and annual oscillation (AO) that would be convolved with those of solar variations in the mesospheric intensities and temperatures; however, the relative contribution of these two may not be decipherable. It can also be seen from Fig. 3c that the power spectral density (PSD) of optical emissions is maximum for the 420 ± 14.8 days, followed by that for SAO (which showed two peaks at 195 ± 3.6 and 150 ± 2.1 days). This is followed by oscillations of 95 ± 0.8 and 84 ± 0.6 days. López-González et al. (2004) presented results from 3 years of data of O_2 and OH emissions and temperatures, wherein they showed a clear AO in temperatures and both AO and SAO of similar magnitudes in the emission rates. Recently, Reid et al. (2014) showed using OH(8–3) night-glow emissions data that the amplitude of the AO dominates that of the SAO. Therefore, the results obtained in this study are in agreement with some of those reported in the literature from other latitudes.

As shown in Fig. 2 and discussed earlier we have observed broad similarities in the variations in O_2 and OH emission intensities which vary with SSN and F10.7 flux. There are, however, occasions when both intensities do not show solar-cycle-related variations, and these are most probably due to altitudinally varying wave activities in the mesosphere. In order to ascertain this, correlation analyses have been carried out between the mesospheric intensities and solar parameters over an interval of a few days. Figure 4a shows 4-day running average of O_2 and OH intensities and SSN in magenta, blue, and green, which show a broad similarity with one another. The 4-day running average was taken to smooth out the night-to-night atmospheric fluctuations in the dataset so that the solar influences, if any, get highlighted. Figure 4b, c, and

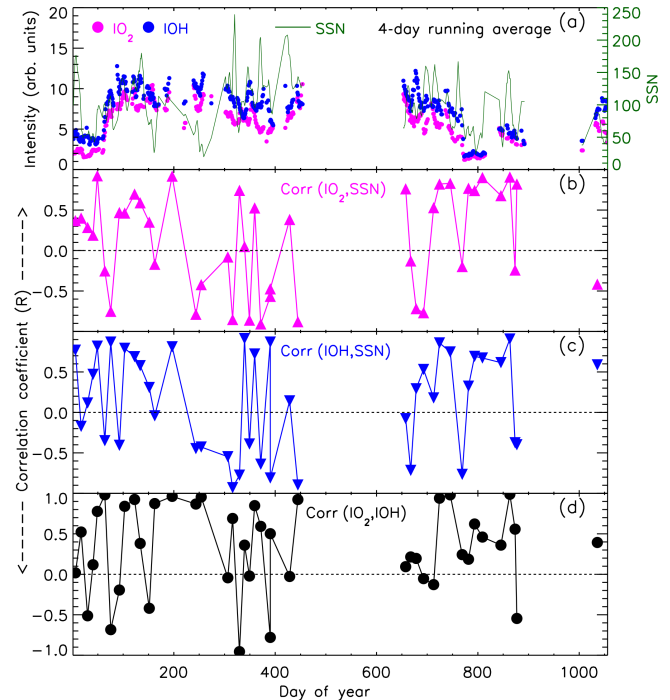


Figure 4. (a) Four-day running averages of O_2 and OH intensities and SSN. Correlation coefficients are shown for the variations obtained between (b) O_2 intensities and SSN, (c) OH intensities and SSN, and (d) O_2 and OH intensities. These correlation coefficients are obtained by considering around 10 days of continuous data of all the parameters.

d respectively show the correlation coefficients of the variability between O_2 intensities and SSN, OH intensities and SSN, and O_2 and OH intensities. These correlation coefficients are obtained by considering around 10 days of continuous data of all the parameters that are shown in Fig. 4a. Thus, a total of 43 values of the correlation coefficients for 437 observational nights of existing data were obtained. The O_2 and OH emissions show positive correlation between them for most of the time during the reported observational period (Fig. 4d). It is also worth noting that the O_2 and OH emissions show similar variations to those in SSN and F10.7 in longer time periods (Fig. 3c); however, as seen in Fig. 4b and c their correlations with SSN are not always good for shorter timescales. It can be seen that when one of the mesospheric intensities (either O_2 or OH) shows poor or anti-correlation with SSN (Fig. 4b, c), they are poorly or anti-correlated amongst themselves as well (Fig. 4d). However, it may be noted that when O_2 and OH intensities show good correlations between themselves, they are also well correlated with SSN. These observations indicate that the altitudinal variations in mesospheric dynamics play a greater role than solar effects in those intervals. These altitudinal variations could be brought about due to dissimilar wave behavior between 94 and 87 km altitudes, or the presence of wind shears in be-

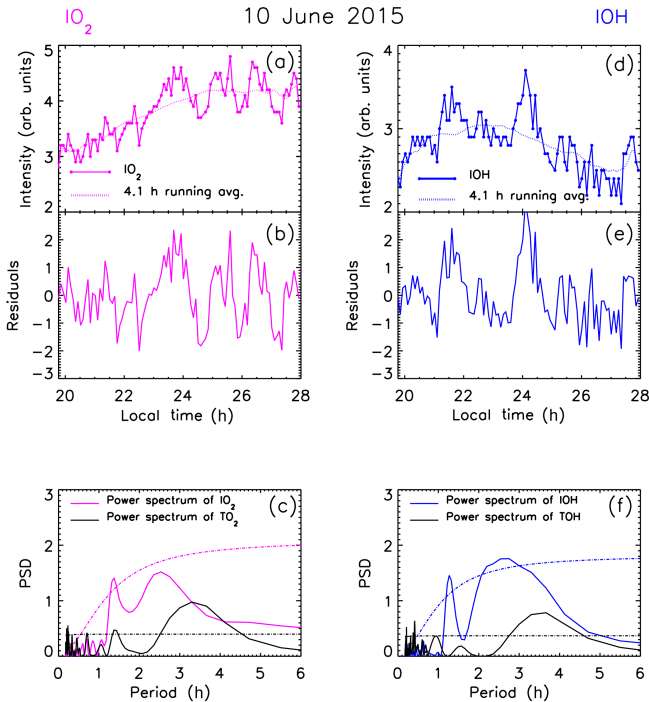


Figure 5. The procedure used to derive gravity wave periodicities from the nocturnal variations in the nightglow intensity data is shown for a sample night of 10 June 2015. **(a, d)** The nocturnal variation in the O_2 and OH emission intensities is shown by the solid lines. Also shown, as dotted lines, are the corresponding 4.1 h running averages of these intensity variations. **(b, e)** Residuals obtained by subtracting the 4.1 h running averaged signal from the original nightglow intensities for both O_2 and OH emissions represented by zero-mean and unit variances. **(c, f)** Lomb–Scargle periodograms of the residuals as shown in **(b, e)**, and the residuals that are obtained using similar procedure but in O_2 and OH temperature variations (not shown) along with 90 % FAL (broken lines) are shown.

tween these altitudes of nightglow emissions. No discernible seasonal effect was noted in the correlation coefficients.

Our study clearly shows that the mesospheric intensity variations are influenced by either variation in solar flux or the local atmospheric dynamics depending on the timescales. In order to understand the fluctuations which are inherent on a given night in O_2 and OH emission intensities, we have calculated the significant periods for each of the 437 nights of observations. In general, the minimum frequency (maximum period) is given by total observational duration. However, we have introduced a more rigorous constraint in deriving the maximum periods in which we have considered that the data should contain at least two cycles. Therefore, we have considered the periods which are smaller than half of the observational duration. Also, the Brunt–Väisälä period at these altitudes is around 5 min, which is equal to the data cadence of our measurement. Thus, the smallest periods of waves that are statistically discernible are ≥ 10 min. The method we followed to derive the periodicities in the nocturnal variations in

the data is depicted in Fig. 5. The nocturnal variations in O_2 and OH intensities are shown by connected lines in Fig. 5a and d, and the dotted lines show the 4.1 h running average of the data for a representative night of 10 June 2015, for which the total duration of data available is around 8.2 h. Therefore, the residuals obtained by subtracting the 4.1 h running average from the original data contain information on the periodicities that are smaller than 4.1 h duration. These are shown in the form of zero-mean unit variances in Fig. 5b and e for O_2 and OH intensities, respectively. This process normalizes the relative power in each period in a given dataset and enables intercomparison of the periodogram of different parameters and of different days (Pallamraju et al., 2010; Singh and Pallamraju, 2016). We have used REDFIT spectral analyses (Schulz and Mudelsee, 2002), which can be performed on unevenly spaced time series and compute a spectral estimate using Welch windowing coupled with the Lomb–Scargle periodogram (Lomb, 1976; Scargle, 1982). The power spectrum of O_2 and OH intensities and corresponding temperatures are shown in Fig. 5c and f using magenta, blue, and black lines. The corresponding broken lines represent the FAL corresponding to the confidence level of 90 %. It can be seen from Fig. 5c that the significant period obtained from IO_2 is of 1.4 h duration and those periods obtained from TO_2 are of 1.4 and 3.2 h duration. Similarly, Fig. 5f shows the presence of periods of 1.3 and 2.5 h duration in IOH and 0.9 and 3.4 h in TOH on the night of 10 June 2015. Similar analysis as demonstrated here for one night has been performed to obtain the dominant periodicities in the O_2 and OH intensities and corresponding temperatures for all the 437 nights of observations. Out of 437 nights of observations, GWs were found to be present on 379 (87 %), 359 (82 %), 412 (94 %), and 401 (92 %) nights in IO_2 , IOH , TO_2 , and TOH , respectively. Waves of periods (of GW regime) are known to play an important role in influencing the mesospheric dynamics (Fritts and Alexander, 2003).

Periods obtained from nocturnal O_2 and OH intensity variations for all the 437 nights are shown in Fig. 6a and d for the years 2013, 2014, and 2015 in red, green, and blue, respectively. As seen in Fig. 5 the periodicities present in O_2 and OH emission intensity variations and corresponding temperatures can be similar or different for the same night due to the presence of the altitude-dependent processes at those altitudes. All the values shown in Fig. 6a and d are independent, and the periods shown are greater than or equal to 10 min and less than or equal to the half of the observational duration. In order to note the broad variations in these GW periods a 30-day running average of these periodicities is performed and is shown in Fig. 6b and e for all the 3 years using same color codes as used in Fig. 6a and d. It should be noted that the GW periods do not show any variation with year (solar cycle).

Estimations for the number of GW occurrences for all the 437 nights of observations have been carried out by summing up all the periods in different bins which are greater than 10 min (frequencies smaller than 6 h^{-1}). Figure 6c and f

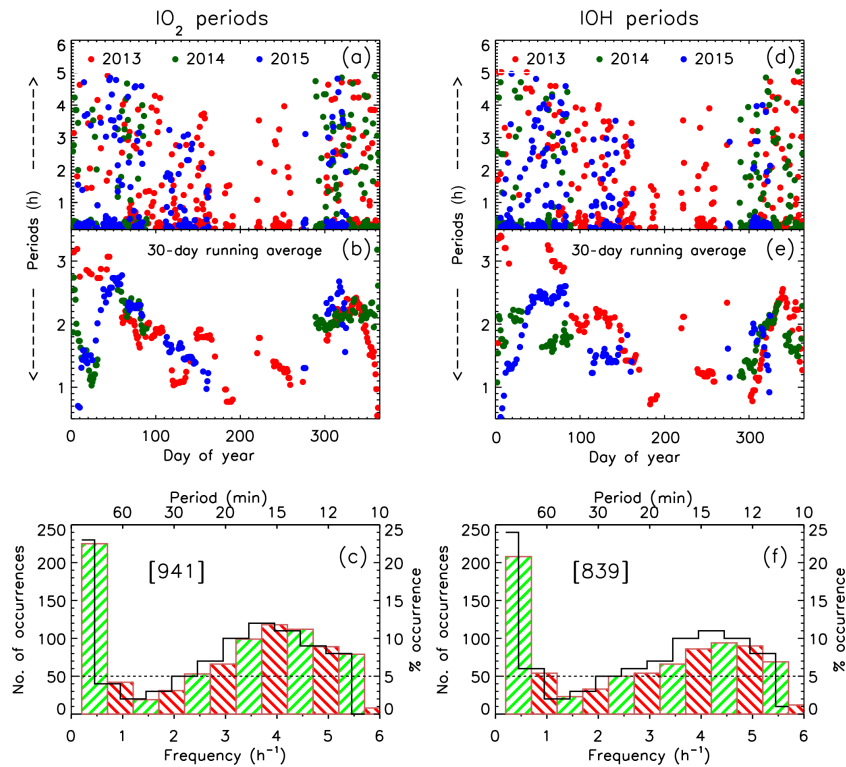


Figure 6. (a, d) Gravity wave periodicities obtained from the O₂ and OH emission intensities for all the 437 nights of observations are shown, which are folded into a 1-year interval. The periods for the year 2013, 2014, and 2015 are shown by red, green, and blue dots, respectively. (b, e) Thirty-day running average of the periods shown in (a, d) are shown for the year 2013, 2014, and 2015. (c, f) Histograms of different periodicities for all nights of observations obtained from the O₂ and OH emission intensity variations as obtained by the method shown in Fig. 5.

show histograms with the number of occurrences of the GW periods as a function of the frequency that were obtained from the O₂ and OH intensity variations, respectively. The temporal scales corresponding to the frequency values are also shown at the top of both Fig. 6c and f. In order to carry out a statistical study for percentage occurrence of fluctuations at any given frequency/time period, histograms have been generated considering a fixed bin size of 0.5 h⁻¹ (i.e., $f \pm 0.25 \text{ h}^{-1}$), which will give rise to varying intervals in the time domain. The histograms shown in black solid lines are the percentage of nights in which waves in a particular frequency bin has occurred. The y axis on the right shows the values corresponding to the percentage of occurrence. From the histograms shown in Fig. 6c and f it can be seen that GW periods observed in both intensities with 11 to 24 min and 2 h periods occur more than 5 % of the observational nights (shown as dotted horizontal line). More than 23 % of nights show the presence of the 2 h duration followed by 12 % of nights with 15 min of periodicities in both mesospheric intensities. It is encouraging to see from the statistics in Fig. 6c and f that the GW periods obtained from the O₂ and OH intensity variations show a similar behavior. The total number of periods (obtained by summing up the number of dots in

Fig. 6a and d) present in O₂ and OH emission intensities for all the 437 nights is 941 and 839 (also shown in Fig. 6c and f).

Similar to the intensities, the GW periodicities obtained from the nocturnal O₂ and OH temperature variations are shown in Fig. 7a and d. The same color code as has been used for the periods obtained from the intensity data (in Fig. 6) is used here as well. As seen from Fig. 7b and e, similar to that of intensities, the temperatures also do not show significant variations in GW periods within the 3 years. The total number of GW periodicities (greater than Brunt–Väisälä period) which are present in O₂ and OH temperatures for all the 437 nights of observations is 1266 and 1214, respectively, which are greater in number as compared to those observed in the intensity variations. The histograms of the periodicities obtained in the O₂ and OH temperatures are shown in Fig. 7c and f, respectively. The GW periodicities obtained from the temperatures data also show the dominance of a 2 h period similar to those observed in the intensities. From Fig. 7 it can be seen that GW periods observed in both O₂ and OH temperatures ranging from 15 min to 2 h occur more than 5 % of the observational nights. More than 18 % of nights show the presence of the 2 h period and around 12 % of nights show the

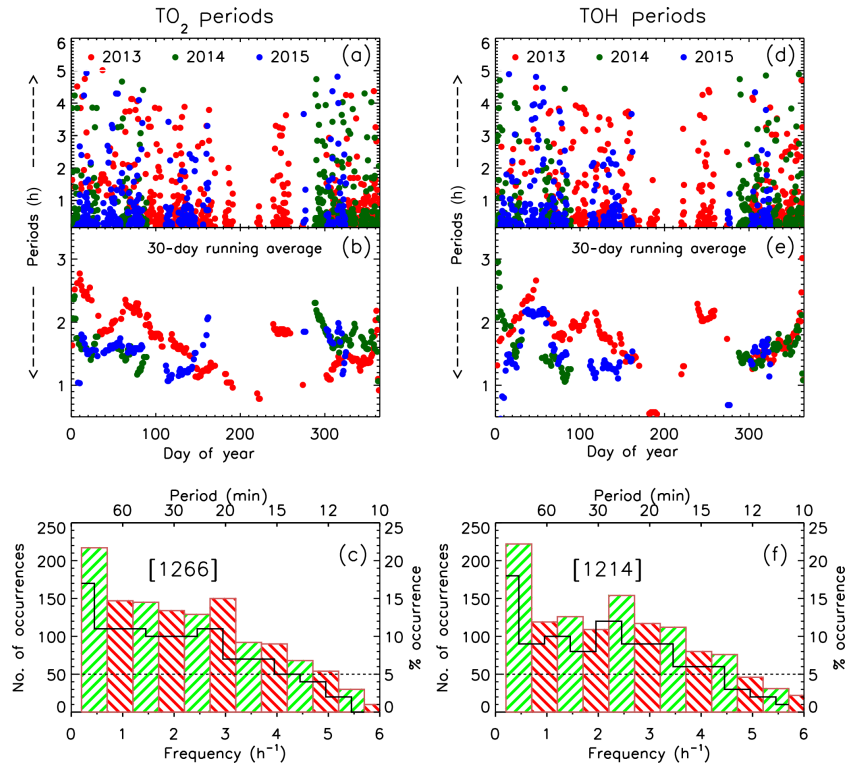


Figure 7. Same as of Fig. 6 but for the temperatures obtained from the $O_2(0-1)$ atmospheric and $OH(6-2)$ band emission intensities.

periodicities with 20 to 60 min in both O_2 and OH temperatures. Hence, it is very clear that the periods obtained from O_2 and OH temperatures show a greater number of larger periodicities than observed in periodicities obtained from intensities. One of the findings of this statistical study is that the GW periods obtained using temperatures do not show a significant number of shorter periodicities (with a period of less than 15 min) as observed in the intensities. Also, it is intriguing as to why the smaller timescales are seen fewer in number as compared to the longer ones in the temperatures. It should be appreciated that intensity variations are due to changes in density of reactants, the temperature of the medium, or pressure waves. In this regard it has been shown that the shorter-period waves are easily discernible in intensities as compared to the corresponding temperatures (Singh and Pallamraju, 2016). The observations described above could be due to the fact that any fluctuations in the densities of reactants will directly affect the emission intensities and thus readily respond to the smaller periods than those in the mesospheric temperatures. Makhlof et al. (1990) showed that temperature variations induced in the nightglow emission are directly proportional to the amplitude of the propagating wave. In the present experiment any wave with temperature fluctuation less than the uncertainty of ± 3 K will not be discernible. However, some of the earlier experiments with simultaneous OH intensities and temperature measurements (e.g., Tepley et al., 1981) also showed that, on a given night, not all the

periods seen in temperatures be present in the intensities, and vice versa. Further, in another result when the periods in intensity and temperature were similar (Taylor et al., 1991), it was shown that the intensity fluctuations lead those in the temperatures. In this background the circumstantial evidence points to inertia of the system and/or amplitude of the temperature that affects the response of smaller periodic fluctuations in temperature variations to be seen readily in those derived from the optical measurements. Further, the fact that longer periodicities in temperatures are seen to a greater extent than the shorter ones confirms this proposition. This is akin to superposition of waves seen in intensities that form a longer time period wave in temperatures. Simulation studies will help in gaining a greater understanding for verifying this conjecture. For longer durations, the inertia of the system is not expected to have any effect and thus, similar to the variability in emission intensities, the temperature variations also show solar-cycle-related periods (Fig. 3).

It can be seen from Figs. 6 and 7 that the longer periods exist during winter months and shorter ones in the summer/monsoon months. However, a closer inspection of Figs. 6 and 7 along with Fig. 1 indicates that this could be an artifact of the shorter observation duration in summer months. In summer nights there is a greater prevalence of clouds. Thus, in order to make a fair judgement on seasonal changes in GW periods, we have to consider data of same duration all through the nights. For this study we have chosen

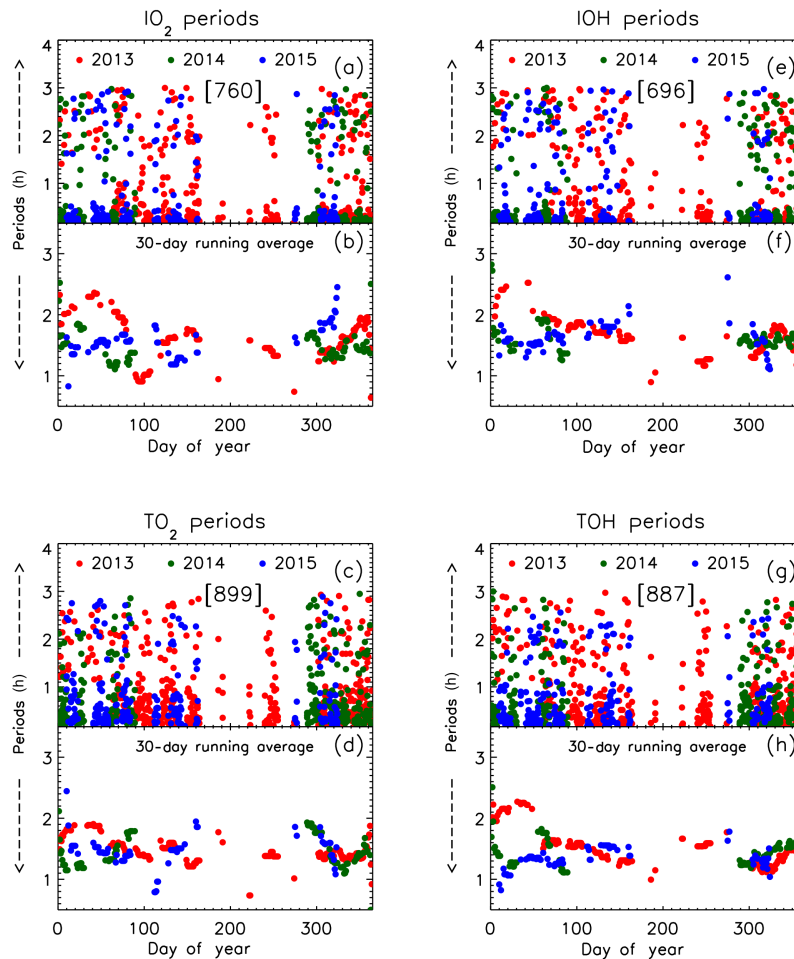


Figure 8. Same as in Figs. 6 and 7a, b, d, and f but for the periods that have been derived from only those nights for which the total duration of observation was greater than 6 h. The periods are obtained by using the same method as illustrated in Fig. 5. The residuals of O_2 and OH intensities and temperatures correspond to the periods that are less than 3 h durations. As can be clearly seen, the GW periods show neither seasonal variations nor solar activity dependence.

only those nights on which the observation time is greater than 6 h, which equates to 350 nights (among 437 nights as seen in Fig. 1). Since we have chosen the nights with more than 6 h of observations, in obtaining the statistics we have considered only those periods which are less than 3 h (half of the observational duration); the procedure for this analysis is similar to that depicted in Fig. 5. The periods obtained in this way in O_2 and OH intensities and related temperatures are shown in Fig. 8 (color codes are similar to those used in Figs. 6 and 7). It can be seen that the GW periods do not show any seasonal variation. This is also confirmed in the 30-day running averages of the periods for all the 3 years of observation, which do not show much variation in their values with respect to seasons. A few earlier studies which dealt with seasonal behavior mainly concentrated on the number of wave occurrences and their propagation and not on the magnitudes of wave periodicities. The present study thus estab-

lishes that the wave periods (in GW regime) in the nighttime mesosphere do not show any seasonal variations.

4 Summary and conclusions

We have presented the long- and short-timescale variations in the mesospheric nightglow emission intensities and corresponding rotational temperatures which have been measured from Gurushikhar, Mount Abu, in India using $O_2(0-1)$ and OH(6-2) band emissions which emanate from 94 and 87 km altitude, respectively. Spectral analyses on 437 nights of observations of O_2 and OH intensities and the corresponding temperatures have been carried out for data during January 2013 to November 2015. Statistically significant periodicities of around 150, 195, 270, and 420 days were obtained. The solar variations in this duration also displayed some of the periodicities (150, 190, 245, 380, and 410 days) that are present in atmospheric oscillations, thereby revealing clear

evidence of solar activity influencing the mesospheric airglow emissions and temperatures. In addition to these common periods, the O₂ and OH intensities also showed periods around 84, 95, and 122 days which are due to the seasonal variations. Not all the periodicities which are present in O₂ and OH intensities are present in temperatures, and vice versa. Although the dominant periods observed in the SSN are present in those of both the mesospheric emission intensities, for some durations the temporal variations in the intensities do not show similarity to that of the solar flux. Therefore, the influence of solar variability on the behavior of mesospheric intensity has been investigated in shorter durations. In order to do that, correlation coefficients have been obtained by considering 10 days of continuous data of O₂ and OH emission intensities and SSN. These analyses showed that O₂ and OH intensity variations are correlated with each other for most of the nights. When they show better correlation between themselves, their correlation with SSN variability is also good, which indicates that the variability in these intensities is being affected by the solar effects. However, when O₂ and OH intensities show poor or anti-correlation between them, in those periods one of these intensities shows poor or anti-correlation with SSN. This indicates that during these periods, altitude-dependent processes, which are due to atmospheric dynamics, play a greater role as compared to the solar influence. GW periodicities have been obtained for all the individual nights using nocturnal variations in the O₂ and OH intensities and corresponding temperatures. A statistical study of these periodicities obtained for all the 437 nights of observations reported here shows significantly different behavior in intensities and temperatures. In intensities it has been observed that GWs show the presence of 2 h and 15 to 20 min periodicities in over 23 and 10 % of nights, respectively. However, temperatures show 2 h and 20 to 60 min periodicities for over 18 and 12 % of nights, and do not show a significant number of periodicities smaller than 15 min. The smaller number of shorter periods seen in temperatures as compared to the intensities is attributed to the time taken for temperatures to respond to the dynamical processes, and/or the wave amplitudes, mainly in the smaller-timescale range. The mesospheric GW periodicities show neither seasonal dependence nor solar activity dependence in their occurrence rate or time periods. Thus, the results of the kind presented in this study provide us with a comprehensive picture of mesospheric wave dynamics in terms of characterizing their response to various sources that give rise to the variability in the mesospheric intensities and temperatures. In addition, these findings would help in modeling studies to better characterize the mesospheric dynamics on large and short timescales.

5 Data availability

The optical data used in this work were obtained by the Physical Research Laboratory and can be made available on request. The sunspot number data were obtained from ftp://ftp.swpc.noaa.gov/pub/indices/old_indices/ and F10.7 data were obtained from ftp://ftp.ngdc.noaa.gov/STP/GEOMAGNETIC_DATA/INDICES/KP_AP/.

Competing interests. The authors declare that they have no conflict of interest.

Acknowledgements. This work is supported by Department of Space, Government of India.

The topical editor, E. Yizengaw, thanks S. Gurubaran and one anonymous referee for help in evaluating this paper.

References

- Batista, P. P., Takahashi, H., and Clemesha, B. R.: Solar cycle and the QBO effect on the mesospheric temperature and nightglow emissions at a low latitude station, *Adv. Space Res.*, 14, 221–224, 1994.
- Bretthorst, G. L.: *Bayesian Spectrum Analysis and Parameter Estimation*, Springer-Verlag, New York, 1988.
- Chowdhury, P., Choudhary, D. P., Gosain, S., and Moon, Y.-J.: Short-term periodicities in interplanetary, geomagnetic and solar phenomena during solar cycle 24, *Astrophys. Space Sci.*, 356, 7–18, 2015.
- Clemesha, B., Takahashi, H., Simonich, D., Gobbi, D., and Batista, P.: Experimental evidence for solar cycle and long-term change in the low-latitude MLT region, *J. Atmos. Sol.-Terr. Phys.*, 67, 191–196, 2005.
- Ejiri, M. K., Shiokawa, K., Ogawa, T., Igarashi, K., Nakamura, T., and Tsuda, T.: Statistical study of short-period gravity waves in OH and OI nightglow images at two separated sites, *J. Geophys. Res.*, 108, 4679, doi:10.1029/2002JD002795, 2003.
- Fritts, D. C. and Alexander, M. J.: Gravity wave dynamics and effects in the middle atmosphere, *Rev. Geophys.*, 41, 1003, doi:10.1029/2001RG000106, 2003.
- Kim, Y. H., Lee, C., Chung, J. -K., Kim, J. -H., and Chun, H.-Y.: Seasonal variations of mesospheric gravity waves observed with an airglow all-sky camera at Mt. Bohyun, Korea (36° N), *Journal of Astronomy and Space Science*, 27, 181–188, doi:10.5140/JASS.2010.27.3.181, 2010.
- Lakshmi Narayanan, V. and Gurubaran, S.: Statistical characteristics of high frequency gravity waves observed by OH airglow imaging from Tirunelveli (8.7° N), *J. Atmos. Sol.-Terr. Phys.*, 92, 43–50, doi:10.1016/j.jastp.2012.09.002, 2013.
- Laskar, F. I., Pallamraju, D., Veenadhari, B., Lakshmi, T. V., Reddy, M. A., and Chakrabarti, S.: Gravity waves in the thermosphere: solar activity dependence, *Adv. Space Res.*, 55, 1651–1659, 2015.
- Lomb, N. R.: Least-squares frequency analysis of unequally spaced data, *Astrophys. Space Sci.*, 39, 447–462, 1976.

- López-González, M. J., Rodríguez, E., Wiens, R. H., Shepherd, G. G., Sargoytchev, S., Brown, S., Shepherd, M. G., Aushev, V. M., López-Moreno, J. J., Rodrigo, R., and Cho, Y.-M.: Seasonal variations of O₂ atmospheric and OH(6–2) airglow and temperature at mid-latitudes from SATI observations, *Ann. Geophys.*, 22, 819–828, doi:10.5194/angeo-22-819-2004, 2004.
- Makhlouf, U., Dewan, E., Isler, J. R., and Tuan, T. F.: On the importance of purely gravitationally induced density, pressure, and temperature variations in gravity waves: their application to airglow observations, *J. Geophys. Res.*, 95, 4103–4111, 1990.
- Meriwether Jr., J. W.: A review of the photochemistry of selected nightglow emissions from the mesopause, *J. Geophys. Res.*, 94, 14629–14646, 1989.
- Nakamura, T., Higashikawa, A., Tsuda, T., and Matsushita, Y.: Seasonal variations of gravity wave structures in OH airglow with a CCD imager at Shigaraki, *Earth Planets Space*, 51, 897–906, 1999.
- Pallamraju, D., Das, U., and Chakrabarti, S.: Short- and long-timescale thermospheric variability as observed from OI 630.0 nm dayglow emissions from low latitudes, *J. Geophys. Res.*, 115, A06312, doi:10.1029/2009JA015042, 2010.
- Pallamraju, D., Baumgardner, J., Singh, R. P., Laskar, F. I., Mendillo, C., Cook, T., Lockwood, S., Narayanan, R., Pant, T. K., and Chakrabarti, S.: Daytime wave characteristics in the lower thermosphere: Results from the Balloon-borne Investigations of Regional-atmospheric Dynamics (BIRD) experiment, *J. Geophys. Res.-Space*, 119, 2229–2242, doi:10.1002/2013JA019368, 2014.
- Pertsev, N. and Perminov, V.: Response of the mesopause airglow to solar activity inferred from measurements at Zvenigorod, Russia, *Ann. Geophys.*, 26, 1049–1056, doi:10.5194/angeo-26-1049-2008, 2008.
- Reid, I. M., Spargo, A. J., and Woihte, J. M.: Seasonal variations of the nighttime O(¹S) and OH(8–3) airglow intensity at Adelaide, Australia, *J. Geophys. Res.-Atmos.*, 119, 6991–7013, doi:10.1002/2013JD020906, 2014.
- Scargle, J. D.: Studies in astronomical time series analysis. II. Statistical aspects of spectral analysis of unevenly spaced data, *Astrophys. J.*, 263, 835–853, 1982.
- Scheer, J., Reisin, E. R., and Mandrini, C. H.: Solar activity signatures in mesopause region temperatures and atomic oxygen related airglow brightness at El Leoncito, Argentina, *J. Atmos. Sol.-Terr. Phys.*, 67, 145–154, 2005.
- Schulz, M. and Mudelsee, M.: REDFIT: Estimating red-noise spectra directly from unevenly spaced paleoclimatic time series, *Comput. Geosci.*, 28, 421–426, 2002.
- Singh, R. P. and Pallamraju, D.: On the latitudinal distribution of mesospheric temperatures during sudden stratospheric warming events, *J. Geophys. Res.-Space*, 120, 2926–2939, doi:10.1002/2014JA020355, 2015.
- Singh, R. P. and Pallamraju, D.: Effect of cyclone Nilofar on mesospheric wave dynamics as inferred from optical nightglow observations from Mount Abu, India, *J. Geophys. Res.-Space*, 121, 5856–5867, doi:10.1002/2016JA022412, 2016.
- Sivakandan, M., Paulino, I., Taori, A., and Niranjana, K.: Mesospheric gravity wave characteristics and identification of their sources around spring equinox over Indian low latitudes, *Atmos. Meas. Tech.*, 9, 93–102, doi:10.5194/amt-9-93-2016, 2016.
- Taylor, M. J., Espy, P. J., Baker, D. J., Sica, R. J., Neal, P. C., and Pendleton Jr., W. R.: Simultaneous intensity, temperature and imaging measurements of short period wave structure in the OH nightglow emission, *Planet. Space Sci.*, 39, 1171–1188, 1991.
- Taylor, M. J., Pendleton Jr., W. R., Clark, S., Takahashi, H., Gobbi, D., and Goldberg, R. A.: Image measurements of short period gravity waves at equatorial latitudes, *J. Geophys. Res.*, 102, 26283–26299, 1997.
- Tepley, C. A., Burnside, R. G., and Meriwether, J. R.: Horizontal thermal structure of the mesosphere from observations of OH(8,3) band emissions, *Planet. Space Sci.*, 29, 1241–1249, 1981.
- Torr, M. R., Torr, D. G., and Laher, R. R.: The O₂ atmospheric 0-0 band and related emissions at night from Spacelab 1, *J. Geophys. Res.*, 90, 8525–8538, 1985.
- Wiens, R. H. and Weill, G.: Diurnal, annual and solar cycle variations of hydroxyl and sodium nightglow intensities in the Europe-Africa sector, *Planet. Space Sci.*, 21, 1011–1027, 1973.